A Quasi-One-Dimensional Integration Technique for the Analysis of Planar Microstrip Circuits via MPIE/MoM

Luciano Tarricone, Mauro Mongiardo, and Francesco Cervelli

***Abstract*—The mixed-potential integral-equation approach, using spatial-domain closed-form Green's functions, and discretized with the method-of-moments, is a state-of-the-art method for the analysis of planar microstrip circuits. One of its most time-demanding tasks is the evaluation of the impedance matrix terms, which typically requires the numerical computation of two-dimensional integrals. A method based on suitable changes of coordinates and domains is introduced in this paper in order to reduce such integrals to a quasi-one-dimensional numerical integration, with a substantial enhancement in the efficiency of the analysis, without affecting the accuracy of the approach. Results are given demonstrating, for practical accuracy values, an improvement of typically one order of magnitude in simulation times.**

I. Introduction

EFFICIENT modeling of printed circuits and antennas is crucial in current microwave engineering [1], [2] and has stimulated several contributions. In particular, a mixed-potential integral equation (MPIE) was proposed by Mosig [3], [4]. More recently, the latter formulation was enhanced by the introduction of suitable closed-form spatial-domain Green's functions [5] and suitable transformations of the impedance matrix [6]. Considerable efforts are currently made in order to improve the efficiency and accuracy of these numerical methods, such as the inclusion of three-dimensional (3-D) unknown currents, efficient choices for the Sommerfeld integration paths [7], and the enhancement of the complex-image method [8], [9] for multilevel stratified microstrip lines [10], [11]. The above-mentioned contributions are mainly in the direction of reducing the computation time required for filling the impedance matrix. Also on this subject, and more recently, papers have been proposed that discuss a clever analysis of basis functions behavior [12], with a significant improvement of space and spectral integrations of coupling integrals [13]–[19].

The numerical core of method-of-moments (MoM) approaches for the analysis of microstrip circuits is represented by both the computation of the impedance matrix and the solution of the corresponding linear system. The computation effort for the evaluation of the impedance matrix is basically determined by the numerical evaluation of some reaction integrals. Therefore, their efficient and accurate solution, possibly appropriate for a wide class of Green's functions, is of paramount importance.

In this paper, we propose an efficient method for evaluating the impedance matrix elements of the circuit via a suitable computation of the relevant reaction integrals. The two-dimensional (2-D) numerical integration encountered in previous approaches [20] is reduced to a quasi-one-dimensional (1-D) numerical integration. Even though this is achieved by partitioning the problem domain into equal cells, this does not represent a practical limitation to the presented technique, as different optimum sizes for the elementary cells can be used in several regions of a single circuit so that an optimum accuracy is ensured. The method proposed is valid for a very large class of Green's function (the only hypothesis is that the Green's function depends only on the source–test distance), and can also be applied to circuits with more than one dielectric layer.

This paper is organized as follows. First, for the reader's convenience, the MPIE formulation is resumed; afterwards, the quasi-1-D integration method is described, some results are given, and finally, conclusions are drawn.

II. Electric–Field MPIE with Closed-Form Green's Functions

We consider N-port planar circuits with infinite transverse dimensions for both the dielectric and ground plane; the metallization thickness is assumed negligible. In order to achieve improved convergence properties, we select the MPIE formulation [3], [4], which is solved by considering closed-form Green's functions in the spatial domain and by using the MoM.

Spatial-domain mixed —potential Green's functions for a layered medium are expressed by Sommerfeld integrals [21] whose integrands are slowly decaying oscillating functions, hence, the calculation is very time consuming. A possible approach to circumvent this problem is the quasi-dynamic image model [22], which is not accurate enough when surface and leaky wave effects must be accounted for [23].

The evaluation of the above-mentioned Green's functions in closed form is performed as suggested in [5], [9], and [24]. Accordingly, the spatial-domain mixed-potential Green's functions are written in the following manner:

$$\begin{aligned} G_{xx}^A &= G_{xx,0}^A + G_{xx,SW}^A + G_{xx,ci}^A \\ G^q &= G_0^q + G_{SW}^q + G_{ci}^q \end{aligned} \tag{1}$$

i.e., as the sum of direct terms and quasi-dynamic images ($G_{xx,0}^A$, G_0^q), surface waves ($G_{xx,SW}^A$, G_{SW}^q), and complex

Manuscript received August 8, 2000.
L. Tarricone and M. Mongiardo are with the Dipartimento di Ingeneria Elettronica e Dell'Informacione, Universita de Perugia, 06125, Perugia, Italy.
F. Cervelli is with Artur Andersen Consulting, Rome 00100, Italy.
Publisher Item Identifier S 0018-9480(01)01687-8.

images ($G^A_{xx,ci}$, G^q_{ci}). As well known, the complex image method is not so accurate when the source–test distance is larger than a certain threshold. This is taken into account by performing a phenomenological analysis, as described in [25]. The same analysis is also useful to cope with some singularity problems, often encountered in space-domain formulations [26].

The Galerkin's MoM is used to discretize the relevant equations, by selecting rooftop functions defined over elementary rectangular domains. This way, a linear system of size N is derived from the MPIE

$$\begin{bmatrix} Z_{xx} & Z_{xy} \\ Z_{yx} & Z_{yy} \end{bmatrix} \begin{bmatrix} I_x \\ Iy \end{bmatrix} = \begin{bmatrix} V_x \\ Vy \end{bmatrix}. \tag{2}$$

The entry Z_{ij} in the impedance matrix $\mathbf{Z}$ is expressed by a fourfold integral, in the spatial variables x', y'—corresponding to the source coordinates—and x, y—corresponding to the test coordinates. Part of its evaluation can be performed analytically [27] and, by paying attention to the choice of appropriate basis functions, the integrals *"can be reduced to double integrals over finite domains"* [20]. The unknowns I_x and I_y are the (complex) amplitudes of the basis functions. The right-hand-side (RHS) vector $[V]$ depends on the excitation applied to the microstrip network.

III. Quasi-1-D Integration

In order to compute the impedance matrix, a time-demanding 2-D numerical integration was employed in earlier methods, even though several efforts have been made to improve the convergence of this computation [27], [20]. Some attempts in this sense have also been made by focusing on appropriate choices of the basis and test functions [28], with attention paid on the meshing performed on the problem's domain. In this last approach [28], the entries of the matrix in (2) are expressed as a four-dimensional (4-D) integral

$$\langle f, G * g \rangle = \int_{D_x} \int_{D_y} f(x, y) \int_{D_{x'}} \int_{D_{y'}} G(r) g(x, y)\, dx'\, dy'\, dx\, dy \tag{3}$$

where D_x, D_y, $D_{x'}$, and $D_{y'}$ are the domains along x, y, x', and y' of the interacting cells (Fig. 1), $r = \sqrt{(x-x')^2 + (y-y')^2}$, and the fourfold integration appearing in (3) is therein transformed into a 2-D one.

In this paper, we show how integration (3) can be reduced to a quasi-1-D integral. The basic observations are: 1) the dependence of the Green's function only on the source–test distance r; 2) the possibility of reducing the remaining terms in the integration kernel (3) to functions with the same behavior; and 3) the possibility of numerically evaluating the contour of the integration domains for the above-mentioned remaining terms. The three observations lead to the following procedure: first, the four integrals can be considered as a 2-D convolution, which can be analytically solved inside each elementary cell of the circuit. This way, (3) is reduced to a 2-D integration, whose kernel is the product between the Green's function and the function attained from the 2-D convolution. A final change of coordinates is now sufficient to separate the two integrals so that one integration is numerically performed with high efficiency by evaluating an analytical function in a small number of points (less than ten). Hence, only a 1-D integration must be performed to completely evaluate (3).

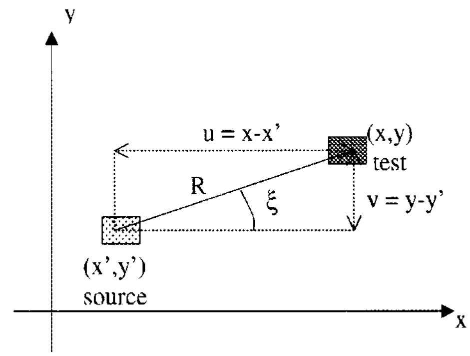

Fig. 1. Reference system and the relative changes of coordinates. One source and one test current cell are sketched.

We continue now to describe with more details the proposed integration technique. The usual change of variables

$$\begin{aligned} x - x' &= u \\ x + x' &= p \\ y - y' &= v \\ y + y' &= q \end{aligned} \tag{4}$$

reduces the problem to a double integration, hence, providing

$$\begin{aligned} &\iint f(x, y) \iint G\left(\sqrt{(x-x')^2 + (y-y')^2}\right) \\ &\quad \cdot g(x', y')\, dx'\, dy'\, dx\, dy \\ &= \frac{1}{4} \iint G(u, v) \iint f\left(\frac{u+p}{2}, \frac{v+q}{2}\right) \\ &\quad \cdot g\left(\frac{p-u}{2}, \frac{q-v}{2}\right) dp\, dq\, du\, dv \end{aligned} \tag{5}$$

(variables x, x', y, y', u, and v are introduced and described in Fig. 1).

Letting D_x be the domain for the x-variable, we can cast

$$S(u, v) \triangleq \frac{1}{4} \int_{D(p)} \int_{D(q)} f\left(\frac{u+p}{2}, \frac{v+q}{2}\right) \cdot g\left(\frac{p-u}{2}, \frac{q-v}{2}\right) dp\, dq. \tag{6}$$

With a suitable change of coordinates (see the Appendix for details), the integration (6) can be transformed into a bidimensional convolution

$$S(u, v) = S(\zeta, \eta) = \int_{D(\zeta)} \int_{D(\eta)} f(\zeta, \eta) g(\zeta - u, \eta - v)\, d\zeta\, d\eta \tag{7}$$

which can be solved very efficiently in analytical form, as described in the Appendix. This way, (3) is transformed into a two-variable integration

$$\int_{D(u)}\int_{D(v)} G(u,\, v)S(u,\, v)\, du\, dv. \tag{8}$$

With the following new change of variables:

$$u = r\cos\xi \quad v = r\sin\xi \tag{9}$$

we can write

$$\int_{D(u)}\int_{D(v)} G(u,\, v)S(u,\, v)\, du\, dv = \int_{r_1}^{r_2} G(r)r \int_{\xi_1(r)}^{\xi_2(r)} S(r\cos\xi,\, r\sin\xi)\, d\xi\, dr. \tag{10}$$

Thanks to the fact that the Green's functions only depend on the source–test distance r, a function $W(r)$

$$W(r) \triangleq \int_{\xi_1(r)}^{\xi_2(r)} S(r\cos\xi,\, r\sin\xi)\, d\xi \tag{11}$$

can be evaluated nearly completely in closed form, with a very high efficiency ($\xi_1(r)$ and $\xi_2(r)$ can be numerically evaluated for each fixed value of r). Finally, we have

$$\iint f(x,\, y) \iint G\left(\sqrt{(x-x')^2 + (y-y')^2}\right) \cdot g(x',\, y')\, dx'\, dy'\, dx\, dy = \int_{r_1}^{r_2} W(r)G(r)r\, dr. \tag{12}$$

With a suitable choice [28] of basis and test functions, $W(r)$ is integrable in the Riemann sense. The $S(u,\, v)$ and $W(r)$, as well as the forms of domains $D(p)$ and $D(q)$, $\xi_1(r)$ and $\xi_2(r)$, and r_1 and r_2 depend on the choice of the basis and test functions and their domain of definition.

After evaluating $W(r)$, the Z-matrix terms can be written as

$$\begin{aligned}
Z_{xx} &= \int \left[W_{1\,x}(r)G^A_{xx}(r) - \frac{1}{\omega^2}\, W_{2x}(r)G^q(r) \right] r\, dr \\
Z_{xy} &= \int \left[-\frac{1}{\omega^2}\, W_{3x}(r)G^q(r) \right] r\, dr \\
Z_{yx} &= \int \left[-\frac{1}{\omega^2}\, W_{3y}(r)G^q(r) \right] r\, dr \\
Z_{yy} &= \int \left[W_{1y}(r)G^A_{yy}(r) - \frac{1}{\omega^2}\, W_{2y}(r)G^q(r) \right] r\, dr
\end{aligned} \tag{13}$$

thus demonstrating that the elements of the impedance matrix can be evaluated by solving a quasi-1-D integral.

The proposed quasi-1-D formulation can be exploited when equal cells are used in a rectangular mesh. An appropriate partitioning of the circuit into subregions can be generally used to analyze every subregion with an optimum cell size. In the Appendix, details are given about the derivation of the coefficients $W_{\{1,\,2,\,3\}\{x,\,y\}}$ for the case of rooftop functions.

As already mentioned, the quasi-1-D approach has been tested here in the case of a Galerkin MoM using rooftop basis and test functions. In the Appendix, the detailed formulation for this case is given. Nevertheless, it can also be extended to other functions, such as pulse functions, attaining different forms for (13).

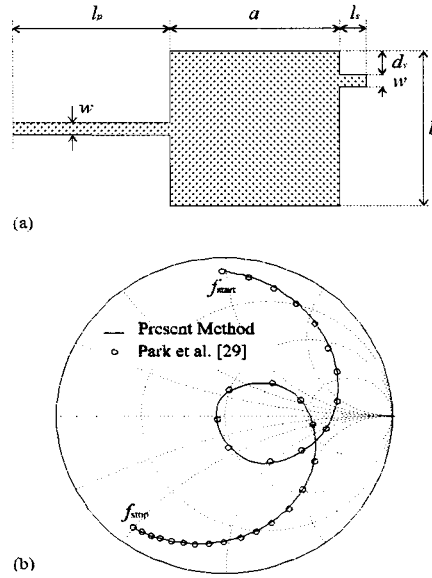

Fig. 2. (b) Input impedance on the Smith chart of: (a) the microstrip-line center-fed square antenna with a tuning stub. Physical dimensions: $\epsilon_r = 2.62$, $d = 0.794$ mm, $a = b = 28.6$ mm, $w = 2.2$ mm, $l_p = 26.4$ mm, $l_s = 4.4$ mm, $d_s = 4.4$ mm. Frequency range: 2.98–3.3 GHz. A mesh with a 3-mm edge was used for the simulations.

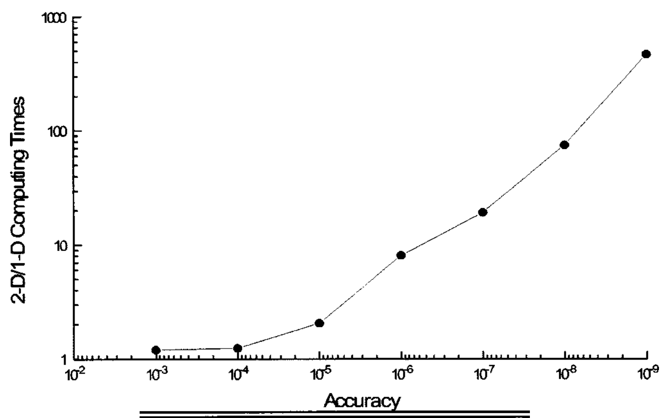

Accuracy	*Error on S parameters*
10^{-8}	0.12%
10^{-7}	0.41%
10^{-6}	0.64%
10^{-5}	1.25%
10^{-4}	1.75%
10^{-3}	3.12%

Fig. 3. Comparison between the 1-D and 2-D integration's performance. Normalized times refer to the analysis of the patch antenna in Fig. 2. They are attained as the ratio between the simulation time of the 2-D and 1-D implementation. On the x-axis, the accuracy required to make the integration converge is reported. An accuracy of 10^{-6} is typically selected for practical computation (refer to table).

IV. Results

The accuracy and efficiency of the implemented method is demonstrated for a patch antenna, reported in the literature and sketched in Fig. 2. In Fig. 3, we compare the time performance

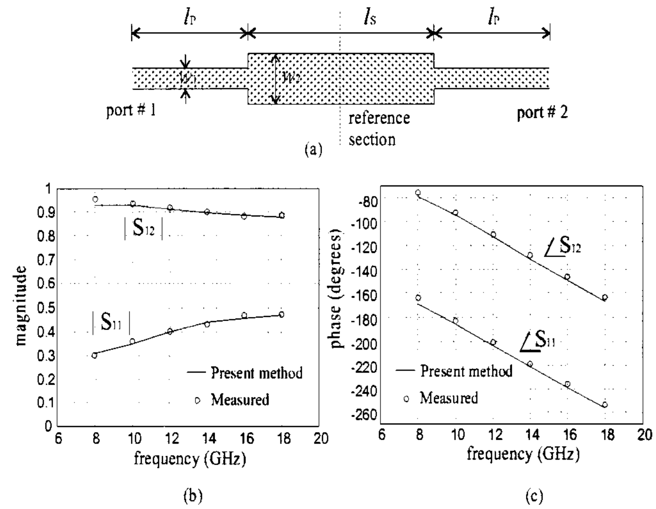

Fig. 4. (a) Scattering parameters of matching section: (b) in magnitude and (c) in phase. Physical dimensions: $\varepsilon_r = 9.9$, $d = 10$ mil, $w_1 = 9.2$ mil, $w_2 = 23$ mil, $l_p = 30$ mil, $l_s = 50.6$ mil. A mesh with a 0.5-mm edge was used for the simulations.

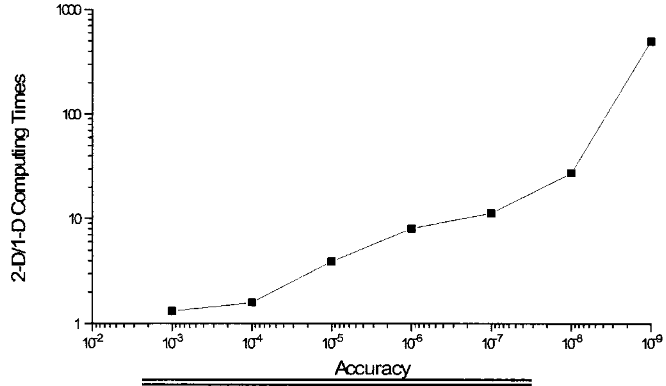

Accuracy	*Error on S parameters*
10^{-8}	0.23%
10^{-7}	0.51%
10^{-6}	0.96%
10^{-5}	1.95%
10^{-4}	2.1%
10^{-3}	2.82%

Fig. 5. As in Fig. 3, referring to the circuit in Fig. 4.

of an MPIE/MoM package implementing a quasi-1-D integration of (3) with respect to the previous 2-D integration proposed by [28]. In the x-axis, the required numerical accuracy is reported, on the y-axis the corresponding normalized computing time for the 2-D implementation with respect to the quasi-1-D one. We define accuracy as the threshold considered to identify the integration convergence. A typical value, guaranteeing a good tradeoff between performance and accuracy is 10^{-6} (errors for scattering parameters are around 1%).

The case of Fig. 2, simulated with a mesh with a 3-mm edge, generates a matrix of dimension 240. When an accuracy of 10^{-6} is considered, the computing time for one frequency point is 2.67 s on a PC Pentium 200 MHz with the 2-D implementation, and 0.33 s using the quasi-1-D integration. A sparse banded approach is used for the system solution step, as described in [6]: it guarantees a high efficiency in the system solution time, taking advantage from the use of reordering techniques.

As easily predictable, the 1-D integration is highly superior. The numerical complexity on the number of integration points is quadratical in the case of the 2-D integration, and linear in the case of quasi-1-D solution. This is in clear accordance with the response of the reported curve.

Another evidence is reported in Fig. 4, where a two-port circuit is analyzed. The advantage of the 1-D integration is also apparent in this case (normalized 2-D/1-D simulation times are reported in Fig. 5). The case of Fig. 4, simulated with a mesh with a 0.5-mm edge, generates a matrix of dimension 416. For an accuracy of 10^{-6}, the computing time for one frequency point is 5.56 s on a PC Pentium 200 MHz with the 2-D implementation, and 0.7 s using the quasi-1-D integration. The sparse banded approach mentioned before is used [6].

The system generation (i.e., the evaluation of the entries in the impedance matrix) is a heavy computational task, as resumed in Table I. For the two circuits (the patch antenna and the two-port circuit), the percentage of time in the two main tasks (system generation and system solution) is reported. As can be seen, the system generation plays an important role. This explains the

TABLE I
EFFORT REQUIRED BY THE SYSTEM GENERATION, WITH RESPECT TO THE SYSTEM SOLUTION AND THE REMAINING TASKS, FOR THE TWO ADDRESSED CASES

Circuit	*System gen.*	*System sol.*	*Other*
PatchAntenna	72%	16%	12%
Two − portCircuit	61%	23%	16%

importance of an efficient solution of (3), as well as the huge speed up achieved with the quasi-1-D integration.

Of course, the reported speed ups are attained when comparing the 2-D implementation with the quasi-1-D implementation of the MPIE/MoM formulation adopted in this paper. Several alternative schemes for the MPIE/MoM are available in the literature. In such cases, the applicability of the proposed strategy should be specifically investigated.

V. Conclusions

In this paper, a substantial enhancement is achieved for the efficient numerical analysis of planar microstrip circuits. A method is described based on suitable analytical changes of coordinates and domains so that the elements are evaluated by solving quasi-1-D numerical integrations instead of the 2-D integrations performed in previous approaches. The above technique, although very general, has been presented in conjunction with an MPIE formulation of the problem, and closed-form spatial-domain Green's function expressions. In such a case, the efficient evaluation of the entries of the impedance matrix is of paramount importance to achieve high performance. Results demonstrate that the proposed approach guarantees a high accuracy and decreases simulation times, in practical cases, typically of one order of magnitude.

Appendix

We describe the case for the xx terms of the impedance matrix; similar formulations hold for the remaining xy, yx, and yy

terms. We refer to the case of basis and test rooftop functions, i.e.,

$$J_{nx} = \begin{cases} \left(1 - \dfrac{|x - x_n|}{h_x}\right), \\ \qquad \text{if } |x - x_n| \le h_x,\ |y - y_n| \le h_y/2 \\ 0, \qquad \text{elsewhere} \end{cases} \tag{14}$$

where $2h_xh_y$ is the surface of the current cell where the function is defined and (x_n, y_n) are the coordinates of the domain's center. Similar expressions hold for the J_{ny}. In the case of rooftop test and basis functions and xx interaction, as seen from (13), we must basically derive two functions W_{1x} and W_{2x}. In fact, the terms $Z_{xxm,n}$ can be expressed as [28]

$$Z_{xxm,n} = \langle J_{xm}, G^A_{xx} * J_{xn}\rangle - \frac{1}{\omega^2}\left\langle \frac{\partial J_{xm}}{\partial x}, G^q * \frac{\partial J_{xn}}{\partial x}\right\rangle. \tag{15}$$

It can be demonstrated that

$$\langle J_{xm}, G^A_{xx} * J_{xm}\rangle = \int_{r_1}^{r_2} W_{1x}(r) G^A_{xx}(r) r\, dr \tag{16}$$

$$\left\langle \frac{\partial J_{xm}}{\partial x}, G^q * \frac{\partial J_{xn}}{\partial x}\right\rangle = -\frac{1}{\omega^2}\int_{r_1}^{r_2} W_{2x}(r) G^q_{xx}(r) r\, dr. \tag{17}$$

Now, in accordance with (11), we indicate with S_{1x} and S_{2x} two functions so that

$$W_{1x}(r) = \int_{\xi_1}^{\xi_2} S_{1x}(r, \xi)\, d\xi \tag{18}$$

$$W_{2x}(r) = \int_{\xi_1}^{\xi_2} S_{2x}(r, \xi)\, d\xi. \tag{19}$$

Therefore, in order to find out W_{1x} and W_{2x}, we must derive the two functions S_{1x} and S_{2x}.

We first concentrate on S_{1x}. Referring to Fig. 6, (3) can be written in the following form, in the case of interaction along the x-axis for both test and basis functions, i.e., for the Z_{xxAB} terms in the impedance matrix:

$$\int_{D(Ay)}\int_{D(Ax)} J_{Ax} \int_{D(By)}\int_{D(Bx)} G(r) J_{Bx}\, dx'\, dy'\, dx\, dy \tag{20}$$

with

$$\begin{aligned} x_A - h_x &\le x \le x_A + h_x \\ x_B - h_x &\le x' \le x_B + h_x \\ y_A - h_y/2 &\le y \le y_A + h_y/2 \\ y_B - h_y/2 &\le y' \le y_B + h_y/2. \end{aligned} \tag{21}$$

By using the change of coordinates (4), we have

$$S_{1x}(u, v) \triangleq \frac{1}{4}\int_{D(p)}\int_{D(q)} J_{Apu}\left(\frac{u+p}{2}, \frac{v+q}{2}\right) cdot J_{Bpu}\left(\frac{p-u}{2}, \frac{q-v}{2}\right) dp\, dq. \tag{22}$$

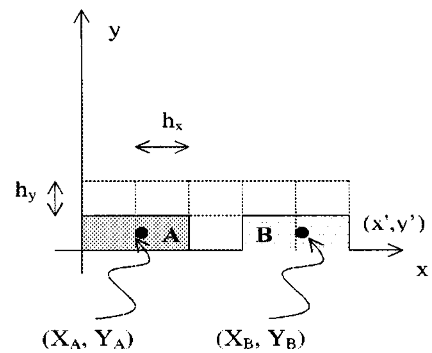

Fig. 6. Simple example for the xx interaction. Two current cells ($\mathbf{A}$ and $\mathbf{B}$) are shown, with the relative centers.

Now, by casting

$$\zeta = \frac{\dfrac{p+u}{2} - x_A}{h_x} \qquad \eta = \frac{\dfrac{p+u}{2} - x_A}{h_x} \tag{23}$$

we have $dp = 2h_x\, d\zeta$, $dq = 2h_y\, dy$, and

$$\frac{\dfrac{p-u}{2} - x_B}{h_x} = \zeta - \frac{u - (x_A - x_B)}{h_x} \tag{24}$$

$$\frac{\dfrac{q-v}{2} - y_B}{h_y} = \eta - \frac{v - (y_A - y_B)}{h_y}. \tag{25}$$

With (23)–(25), (22) is turned into

$$\begin{aligned} S_{1x}(u, v) &= S(\zeta, \eta) \\ &= \int_{D(\zeta)}\int_{D(\eta)} f(\zeta, \eta) g(\zeta - u, \eta - v)\, d\zeta\, d\eta \end{aligned} \tag{26}$$

with

$$\begin{aligned} -2h_x &\le \zeta \le 2h_x \\ -h_y &\le \eta \le h_y. \end{aligned} \tag{27}$$

Now, (26), in the case of xx interactions, can be reduced after some long calculations to the summation of several terms, basically of the following two kinds:

$$2h_y\left(\int_{f(u)}^{0} f'(\zeta) f''(\zeta)\, d\zeta\right)$$

$$2h_y\left(\int_{0}^{g(u)} g'(\zeta) g''(\zeta)\, d\zeta\right) \tag{28}$$

$f(u)$ and $g(u)$ have forms such as

$$1 \pm 2h_x \pm u \tag{29}$$

while $f'(\zeta)$, $f''(\zeta)$, $g'(\zeta)$, and $g''(\zeta)$ have forms such as

$$1 \pm \frac{\zeta}{2h_x}. \tag{30}$$

The solution of (28) with (29) and (30) leads to the following generical solution for (26):

$$S_{1x}(u, v) = (a_3u^3+a_2u^2+a_1u+a_0)(b_3v^3+b_2v^2+b_1v+b_0). \tag{31}$$

The best way to derive the coefficients a_i and b_i in (31) is to recall that (26) is a bidimensional convolution of two rooftop functions. If we indicate with z the distance between two interacting elementary cells, the solution of the convolution with graphical methods easily leads to the following formula:

$$S_{1x}(u, v) = h_x h_y R_{\zeta\zeta}\left(u-\frac{x_A-x_B}{h_x}\right) R_{\eta\eta}\left(v-\frac{x_A-x_B}{h_y}\right) \tag{32}$$

$R_{\zeta\zeta}(z)$ being the convolution along ζ, and $R_{\eta\eta}(z)$ being the convolution along η, with

$$R_{\zeta\zeta} = \begin{cases} \frac{z^3}{6}+z^2+2z+4/3, & -2 \le z \le -1 \\ -\frac{z^3}{2}-z^2+2/3, & -1 \le z \le 0 \\ \frac{z^3}{2}-z^2+2/3, & 0 \le z \le 1 \\ -\frac{z^3}{6}+z^2-2z+4/3, & 1 \le z \le 2 \\ 0, & \text{elsewhere} \end{cases} \tag{33}$$

$$R_{\eta\eta} = \begin{cases} z+1, & -1 \le z \le 0 \\ 1-z, & 0 \le z \le 1 \\ 0, & \text{elsewhere.} \end{cases} \tag{34}$$

Therefore, it is apparent that the coefficients a_i and b_i assume different values depending on the mutual distance z between the interacting cells, even though their form is analytically determined. For instance, using (9), for two cells with $z = 1$, we have

$$\begin{aligned} S_{1x}(r, \xi) = h_x h_y \Bigg(1/2\left(\frac{r\sin\xi-(x_A-x_B)}{h_x}\right)^3 \\ -\left(\frac{r\sin\xi-(x_A-x_B)}{h_x}\right)^2+2/3\Bigg) \\ \cdot\left(1-\frac{r\cos\xi-(y_A-y_B)}{h_y}\right). \end{aligned} \tag{35}$$

Once the S_{1x} has been determined, the W_{1x} is easily evaluated. In fact, we can now observe in (18) that S_{1x} is composed of terms $\cos^m\xi$ and $\sin^n\xi$, with $m, n = 0, 1, 2, 3$, whose primitives are known in closed form. For each value of r, $\xi_1(r)$ and $\xi_2(r)$ can be numerically evaluated: as apparent from Fig. 1, with simple calculations, the values for ξ can be found for all the interacting cells. Moreover, inside each cell the appropriate a_i and b_i can be identified with (32) to perform the integration. The domain of S_{1x} can be partitioned into eight subdomains [the four partitions of $R_{\zeta\zeta}$ in (33) and the two of $R_{\eta\eta}$ in (34)], and the calculation to evaluate W_{1x} become extremely fast.

In conclusion, $W_{1x}(r)$ is evaluated in a very efficient and nearly completely analytical way. Similar procedures can be followed to evaluate $W_{2x}(r)$. It can be derived that

$$S_{2x}(u, v) = \frac{h_y}{h_x} R_{\zeta\zeta}\left(u-\frac{x_A-x_B}{h_x}\right) R_{\eta\eta}\left(v-\frac{y_A-y_B}{h_y}\right). \tag{36}$$

$R_{\zeta\zeta}(z)$ being the convolution along ζ and $R_{\eta\eta}(z)$ being the convolution along η with

$$R_{\zeta\zeta} = \begin{cases} -z-2, & -2 \le z \le -1 \\ 3z+2, & -1 \le z \le 0 \\ -3z+2, & 0 \le z \le 1 \\ z-2, & 1 \le z \le 2 \\ 0, & \text{elsewhere} \end{cases} \tag{37}$$

$$R_{\eta\eta} = \begin{cases} z+1, & -1 \le z \le 0 \\ 1-z, & 0 \le z \le 1 \\ 0, & \text{elsewhere.} \end{cases} \tag{38}$$

The use of (9) transforms S_{2x} into a summation of terms $\cos^m\xi$ and $\sin^n\xi$ with $m, n = 0, 1, 2, 3$ (as in the previous case), whose primitives are known in closed form, thus making the derivation of W_{2x} quite immediate.

REFERENCES

[1] R. Sorrentino, Ed., *Numerical Methods for Passive Microwave and Millimeter Wave Structures*. New York: IEEE Press, 1989.

[2] T. Rozzi and M. Mongiardo, *Open Electromagnetic Waveguides*. London, U.K.: IEE Press, 1997.

[3] J. R. Mosig and F. E. Gardiol, "General integral equation formulation for microstrip antennas and scatterers," *Proc. Inst. Elect. Eng.*, pt. H, vol. 132, pp. 424–432, Dec. 1985.

[4] J. R. Mosig, "Arbitrarily shaped microstrip structures and their analysis with a mixed potential integral equation," *IEEE Trans. Microwave Theory Tech.*, vol. 36, pp. 314–323, Feb. 1988.

[5] G. Dural and M. I. Aksun, "Closed-form Green's functions for general sources and stratified media," *IEEE Trans. Microwave Theory Tech.*, vol. 43, pp. 1545–1552, July 1995.

[6] A. Caproni, F. Cervelli, M. Mongiardo, L. Tarricone, and F. Malucelli, "Bandwidth reduced full-wave simulation of planar microstrip circuits," *Int. J. Appl. Comput. Electromag. Soc.*, vol. 13, no. 2, pp. 197–204, 1998.

[7] P. Gay-Balmaz and J. R. Mosig, "Three dimensional planar radiating structures in stratified media," *Int. J. Microwave Millimeter-Wave Computer-Aided Eng.*, vol. 37, pp. 330–343, Sept. 1997.

[8] D. G. Fang, J. J. Yang, and G. Y. Delisle, "Discrete image theory for horizontal electric dipoles in a multilayered medium," *Proc. Inst. Elect. Eng.*, pt. H, vol. 135, pp. 297–303, 1988.

[9] Y. L. Chow, J. J. Yang, D. G. Fang, and G. E. Howard, "A closed-form spatial Green's function for thick microstrip substrate," *IEEE Trans. Microwave Theory Tech.*, vol. 39, pp. 588–592, Mar. 1991.

[10] C. H. Chan and R. A. Kipp, "Application of the complex image method to the multilevel, multiconductor microstrip lines," *Int. J. Microwave Millimeter-Wave Computer-Aided Eng.*, vol. 7, pp. 359–367, Sept. 1997.

[11] C. H. Chan and R. A. Kipp, "Application of the complex image method to the characterization of microstrip vias," *Int. J. Microwave Millimeter-Wave Computer-Aided Eng.*, vol. 7, pp. 368–379, Sept. 1997.

[12] T. Vaupel and T. Hansen, "Effective spectral domain analysis of planar circuits with different kinds of expansion functions on rectangular subdomains," *Int. J. Microwave Millimeter-Wave Computer-Aided Eng.*, vol. 7, pp. 455–467, Nov. 1997.

[13] L. Alatan, M. I. Aksun, K. Mahadevan, and M. T. Birand, "Analytical evaluation of the MoM matrix elements," *IEEE Trans. Microwave Theory Tech.*, vol. 44, pp. 519–525, Apr. 1996.

[14] N. Kinayman, G. Dural, and M. I. Aksun, "A numerically efficient technique for the analysis of slots in multilayered media," *IEEE Trans. Microwave Theory Tech.*, vol. 46, pp. 430–432, Apr. 1998.

[15] J. X. Zheng, "Three-dimensional electromagnetic simulation of electronic circuits of general shape," *Int. J. Microwave Millimeter-Wave Computer-Aided Eng.*, vol. 4, no. 4, pp. 384–395, 1994.

[16] D. C. Chang and J. X. Zheng, "Electromagnetic modeling of passive circuits elements in MMIC," *IEEE Trans. Microwave Theory Tech.*, vol. 40, pp. 1741–1747, Sept. 1992.

[17] J. Sercu, N. Fache', F. Libbrecht, and P. Lagasse, "Mixed potential integral equation technique for hybrid microstrip-slotline multilayered circuits using a mixed rectangular-triangular mesh," *IEEE Trans. Microwave Theory Tech.*, vol. 43, pp. 1162–1172, Sept. 1992.

[18] T. F. Eibert and V. Hansen, "3-D FEM/BEM hybrid approach based on a general formulation of Huygens' principle for planar layered media," *IEEE Trans. Microwave Theory Tech.*, vol. 45, pp. 1105–1112, July 1997.

[19] T. Vaupel and V. Hansen, "Electrodynamic analysis of combined microstrip and coplanar/slotline structures with 3-D components based on a surface/volume integral equation approach," *IEEE Trans. Microwave Theory Tech.*, vol. 47, pp. 1788–1800, Sept. 1999.

[20] M. I. Aksun and R. Mittra, "Estimation of spurious radiation from microstrip etches using closed-form Green's functions," *IEEE Trans. Microwave Theory Tech.*, vol. 40, pp. 2063–2070, Nov. 1992.

[21] A. Sommerfeld, *Partial Differential Equations in Physics*. New York: Academic, 1949.

[22] Y. L. Chow, "An approximate dynamic spatial Green's function in three dimensions for finite length microstrip lines," *IEEE Trans. Microwave Theory Tech.*, vol. MTT-28, pp. 393–397, MONTH 1980.

[23] J. R. Mosig and F. E. Gardiol, "A dynamical radiation model for microstrip structures," in *Advanced in Electronics and Electron Physics*. New York: Academic, 1982, vol. 59, pp. 175–182.

[24] M. I. Aksun and R. Mittra, "Derivation of closed-form Green's functions for a general microstrip geometry," *IEEE Trans. Microwave Theory Tech.*, vol. 40, pp. 2055–2062, Nov. 1992.

[25] F. Cervelli, M. Mongiardo, and L. Tarricone, "Efficient phenomenologically-based 1-D evaluation of the impedance matrix in a MPIE analysis of planar microstrip circuits," in *Proc. IEEE MTT-S Symp. Dig.*, 1998, pp. 1559–1562.

[26] F. J. Demuynck, G. A. E. Vandenbosch, and A. R. Van de Capelle, "The expansion wave concept—Part I: Efficient calculation of Spatial Green's functions in a stratified dielectric medium," *IEEE Trans. Antennas Propagat.*, vol. 46, pp. 397–406, Mar. 1998.

[27] L. Barlatey, J. R. Mosig, and T. Sphicopoulos, "Analysis of stacked microstrip patches with a mixed potential integral equation," *IEEE Trans. Microwave Theory Tech.*, vol. 38, pp. 608–615, May 1990.

[28] M. I. Aksun and R. Mittra, "Choices of expansion and testing functions for the method of moments applied to a class of electromagnetic problems," *IEEE Trans. Microwave Theory Tech.*, vol. 41, pp. 503–508, Mar. 1993.

[29] I. Park, R. Mittra, and M. I. Aksun, "Numerically efficient analysis of planar microstrip configurations using closed-form Green's functions," *IEEE Trans. Microwave Theory Tech.*, vol. 43, pp. 394–400, Feb. 1995.

Luciano Tarricone was born in Galatone (Lecce), Italy, on May 24, 1966. He received the Laurea degree in electronic engineering (with honors) and the Ph.D. degree from the Rome University "La Sapienza," Rome, Italy, in 1989 and 1994, respectively. Both his Laurea thesis and his Ph.D. dissertation were focused on the biological effects of electromagnetic fields and electromagnetic compatibility.

In 1990, he was a Visiting Researcher at the Italian National Institute of Health Laboratories, where he was in charge of European draft standards for electromagnetic interferences (EMIs) with implanted devices. From 1990 to 1992, he was a Researcher at the IBM Rome Scientific Centers. From 1992 to 1994, he was with the IBM European Center for Scientific and Engineering Computing, Rome, italy, where he was involved in supercomputing for several scientific applications. Since 1994, he has been a Researcher at the Dipartimento di Ingeneria Elettronica e Dell'Informacione, Universita de Perugia, Perugia, Italy, where, since 1998, he has been a Professore Incaricato of electromagnetic fields and electromagnetic compatibility. His main contributions are in the modeling of microscopic interactions of electromagnetic fields and biosystems, and in numerical methods for efficient computer-aided design (CAD) of microwave circuits and antennas. He is currently involved in the finite-difference time-domain analysis of human–antenna interaction, graph-theory methods for the enhancement of numerical electromagnetic techniques, novel CAD tools and procedures for millimeter-wave circuits, and electromagnetic parallel computing. He has authored approximately 110 scientific papers.

Mauro Mongiardo received the Laurea degree (*summa cum laude*) from the University of Rome, Rome, Italy, in 1983, and the Ph.D. degree from the University of Bath, Bath, U.K., in 1991.

He is currently an Associate Professor at the Universita de Perugia, Perugia, Italy. He has been a Visiting Scientist at the University of Victoria, Victoria, BC, Canada, the University of Bath, Oregon State University, Corvallis, and the Technical University of Munich, Munich, Germany. His main contributions are in the area of modeling of waveguide discontinuities, both in the cases of closed and open waveguides, such as microstrip lines or coplanar waveguides. His research interests include numerical methods with contributions in the areas of mode-matching techniques, integral equations, variational techniques, finite-difference time-domain, transmission-line matrix (TLM), and finite-element methods (FEMs). His is also involved with frequency- and time-domain analysis of monolithic microwave integrated circuits (MMICs) and is currently interested in the modeling and computer-aided procedures for the design of microwave and millimeter-wave components.

Francesco Cervelli received the electronic engineering degree (*summa cum laude*) from the Universita de Perugia, Perugia, Italy, in 1997.

In 1998, he joined Artur Andersen Consulting, Rome, Italy, where he is currently a System Engineer.